

EFFECTS OF CASTING PRACTICE ON
MACROSEGREGATION AND MICROSTRUCTURE
OF 2024 ALLOY BILLET

R. C. Dorward and D. J. Beerntsen

Center for Technology
Kaiser Aluminum
P.O. Box 877
Pleasanton, CA 94566Abstract

2024 alloy billets were cast using various drop rates, metal temperatures and mold water flow rates. Of these variables, casting speed (drop rate) had the greatest effect on macrosegregation and microstructure. Fast drop rates generate deep sumps that promote the collection of "isothermal" aluminum-rich dendrites at the ingot center, resulting in solute depletion and duplex, heterogeneous microstructures at this location. Slow casting speeds provide more uniform microstructures and much flatter segregation profiles, in which the alloying element concentrations can be a maximum at the ingot center. Differential scanning calorimetry was used to correlate melting thermograms with the microstructural features of the as-cast and homogenized billets.

Introduction

An experimental program was undertaken to determine the effects of metal temperature, casting speed and mold water flow rate on thermal profiles, microstructures, and macrosegregation in 40 cm diameter 2024 billet. The modeled and measured thermal data agreed closely and were reported previously⁽¹⁾. The major effects of the casting variables are listed in Table I and are summarized

below:

- Increasing the casting speed markedly increases the sump depth and also increases the solidification (cooling) rate. Since a deeper sump allows for more circulation and longer residence times for free-floating "isothermal" dendrites (aluminum-rich primaries), greater macrosegregation would be expected in high drop rate ingots. Dendrite arm spacings should be somewhat smaller.
- Lower metal superheat results in a more isothermal sump with lower thermal gradients. This may be more conducive to the growth of floating "isothermal" primaries, leading to more macrosegregation. Metal superheat has little effect on solidification rate; lower metal temperature reduces sump depth slightly at high mold water rates.
- Higher water flow gives a slightly cooler sump with greater cooling in the mold region, but has little effect on solidification rate. Higher water flow decreases sump depth slightly at low metal superheat.

Table I. Effect of Casting Variables on Sump Depth, Temperature Gradients and Solidification Rate of 40 cm Diameter 2024 Billet

| Casting Speed (cm/min) | Water Flow (l/min) | Metal Temp. at Trough (°C) | Metal Temp. at Mold Top (°C) | Sump Depth (cm) ^a | Average Sump Gradient (°C/cm) ^a | | Mushy Zone Gradient (°C/cm) ^a | | Solidification Rate (°C/sec) ^b | |
|------------------------|--------------------|----------------------------|------------------------------|------------------------------|--|-----|--|------|---|------|
| | | | | | D/4 | D/2 | D/4 | D/2 | D/4 | D/2 |
| 6.35 | 550 | 715 | 696 | 20 | 6.2 | 2.9 | 37.5 | 29.7 | 3.97 | 3.15 |
| 3.8 | 550 | 715 | 678 | 10 | 5.8 | 3.5 | 48.8 | 29.2 | 3.09 | 1.84 |
| 6.35 | 230 | 715 | 694 | 20 | 5.2 | 2.8 | 34.7 | 30.2 | 3.67 | 3.20 |
| 3.8 | 230 | 715 | 672 | 10 | 4.8 | 3.4 | 47.9 | 29.0 | 2.35 | 1.84 |
| 6.35 | 550 | 660 | 645 | 19 | 0.8 | 0.4 | 37.1 | 29.4 | 3.93 | 3.11 |
| 3.8 | 550 | 660 | 641 | 8 | 0.6 | 0.4 | 48.6 | 29.4 | 3.08 | 1.87 |
| 6.35 | 230 | 660 | 645 | 21 | 0.7 | 0.3 | 35.1 | 31.6 | 3.71 | 3.34 |
| 3.8 | 230 | 660 | 642 | 9.5 | 0.8 | 0.5 | 47.1 | 29.7 | 2.98 | 1.88 |

^a Measured values⁽¹⁾^b Calculated from mushy zone gradient and casting speed. For 2024 alloy, which has a freezing range of about 140°C, a solidification rate of 3°C/sec corresponds to a solidification time of ~45 sec.

To assess the effects of these factors on ingot structure, billet slices were examined for composition profiles and macro and microstructural evaluation. Selected billet samples were also analyzed by differential scanning calorimetry (DSC) in the as-cast and homogenized conditions.

Experimental

The casting configuration was a typical level feed, reservoir top DC semi-continuous system with an insulating orifice plate above the aluminum mold. A water ring cooled the mold and sprayed cooling water (at 16°C) on the ingot as it emerged from the mold, thereby providing both primary and secondary cooling of the ingot. Two pairs of 40 cm diameter ingots were cast using molds set up in tandem with one having a water flow rate of 550 l/min, and the other at 230 l/min. Midway through each drop the casting rate was decreased from 6.35 cm/min to 3.8 cm/min. A trough metal temperature difference of about 55°C (715°C vs. 660°C) between the two drops was achieved. The compositions of the two drops are given in Table II.

Table II. Chemical Compositions of 2024 Alloy Billets

| Metal Temp (°C) | Si | Fe | Cu | Mn | Mg | Zn | Ti |
|-----------------|------|------|------|------|------|------|------|
| 715 | 0.11 | 0.21 | 4.68 | 0.61 | 1.35 | 0.09 | 0.01 |
| 660 | 0.11 | 0.21 | 4.68 | 0.67 | 1.35 | 0.09 | 0.01 |

For structural examination, ingot slices were sawed at the 80 cm (6.35 cm/min) and 200 cm (3.8 cm/min) locations. They were evaluated for composition profiles (Quantometer analyses at 12.5 mm increments from surface to center, and inductively coupled plasma spectroscopy (ICPS) at D/4 and D/2), and microstructure at D/4 and D/2 locations in the stress relieved (345°C for 2 hr) and homogenized (495°C for 16 hr, cold water quench) conditions.

The differential scanning calorimetry (DSC) studies were conducted with a Perkin Elmer DSC-4 instrument using heating rates of 20°C/min from 490°C (stress-relieved) and 440°C (homogenized). The stress-relieved samples weighed 31-33 mg; homogenized samples were 108-110 mg.

Results

Macrosegregation

Typical macrosegregation profiles showing the effect of casting speed are plotted in Figure 1. Billets cast at 6.35 cm/min showed the characteristic decrease in composition at the center. With the slower 3.8 cm/min drop rate, the magnesium profiles were fairly flat. The copper profiles, however, showed a reproducible minimum about 15 cm from the surface (D/2.7), and the center concentration was often higher than at any other point in the cross-section. The macrosegregation data obtained by Quantometer analyses are summarized in Table III in the form of a macrosegregation index defined by

$$\text{Index} = \left(\frac{C_{\text{max}} - C_{\text{min}}}{C_{\text{ave}}} \right) 100$$

Note that this index does not identify the type of profile, i.e., maximum or minimum at billet center. Nevertheless, the numbers show considerably higher segregation levels in ingots cast at 6.35 cm/min than at 3.8 cm/min. There did not appear to be any consistently significant effect of the other casting variables.

Because of the unique composition profiles in the billets cast at the slow casting speed, we also determined by ICP analysis the ratio of the compositions at the 11.5 cm and 19.5 cm locations, i.e., approximately D/3.5 and D/2 where concentrations are typically a maximum and a minimum, respectively. These data show essentially identical compositions at both locations in all the 3.8 cm/min drop rate ingots. The billets cast at 6.35 cm/min were more typical, with the most segregation evident for the low metal temperature (660°C) and low water flow (230 l/min) conditions. The lower water flow also appeared to have a positive effect with the higher metal superheat.

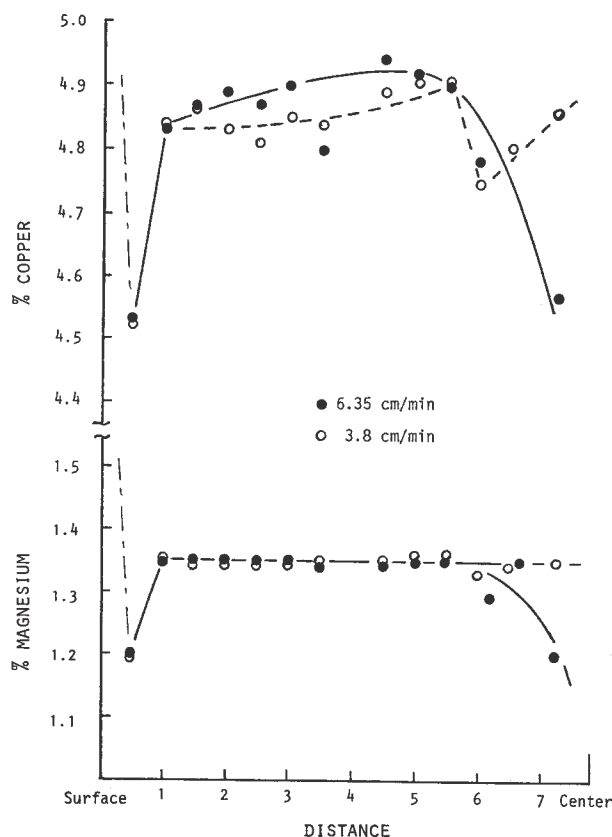


Figure 1. Effect of casting speed on macrosegregation profiles in 2024 billet cast using 715°C metal temperature.

Table III. Effect of Casting Conditions on Macrosegregation in 40 cm Diameter 2024 Billet

| Casting Speed (cm/min) | Water Flow (l/min) | Trough Metal Temp. (°C) | Macrosegregation Index ^a | | Macrosegregation Ratio ^b | |
|------------------------|--------------------|-------------------------|-------------------------------------|------|-------------------------------------|------|
| | | | Cu | Mg | Cu | Mg |
| 6.35 | 550 | 715 | 8.2 | 7.5 | 1.04 | 1.02 |
| 3.8 | 550 | 715 | 4.8 | 3.2 | 0.99 | 0.99 |
| 6.35 | 230 | 715 | 7.7 | 11.4 | 1.08 | 1.06 |
| 3.8 | 230 | 715 | 3.3 | 2.2 | 0.99 | 0.98 |
| 6.35 | 550 | 660 | 6.9 | 7.5 | 1.04 | 1.02 |
| 3.8 | 550 | 660 | 3.5 | 2.3 | 0.99 | 0.99 |
| 6.35 | 230 | 660 | 8.9 | 9.8 | 1.15 | 1.12 |
| 3.8 | 230 | 660 | 4.8 | 3.0 | 0.97 | 0.98 |

^a $(C_{max} - C_{min}) \div C_{ave} \times 100$ by Quantometer.

^b $C(D/3.5) \div C(D/2)$ by ICPS.

Microstructure

Metallographic samples from the D/4 and D/2 locations were examined in stress relieved and homogenized conditions. A 5 sec Keller's etch was used to reveal the as-cast dendrite structure as shown in Figure 2. These low-magnification photomicrographs show the most obvious microstructural effect of changing the casting speed: the faster drop rate resulted in a marked duplex structure consisting of coarse and fine dendrite arm spacings at the ingot center. The coarse dendrites are presumably "isothermal" primaries that collect in the deep sump generated by the high drop rate. Since they are relatively solute-depleted, the average composition at the ingot center is low in copper and magnesium. The phenomenon is minimized when the sump depth is shallower, and the macrosegregation profiles become more "normal", i.e., the last metal to solidify is rich in solute. Because of the bimodal distribution in dendrite arm spacings, we did not make any quantitative measurements of their average dimensions.

The largest and most obvious isothermal dendrites were observed in billets cast at 6.35 cm/min with the low superheat. Their secondary dendrite arm spacing was about 120 μm, indicating a local cooling rate below 0.1°C/sec⁽³⁾, which is more than an order of magnitude lower than that estimated from the casting speed and the mushy zone thermal gradient (Table I). Discounting the coarse dendrites, the remaining structure was somewhat finer in the billets cast at the higher drop rate (~40 vs 60 μm), which corresponds to a faster solidification rate. The microstructural variation associated with the duplex structure in the billets cast at 6.35 cm/min is shown in Figure 3. As noted above, the coarse dendrites are solute-poor and constituent depleted, whereas the fine dendrites (the last to solidify) are rich in constituent phases.

The dendrite structure at the quarter point (D/4) location in all the billets was much more uniform than at the center of the 6.35 cm/min drop rate

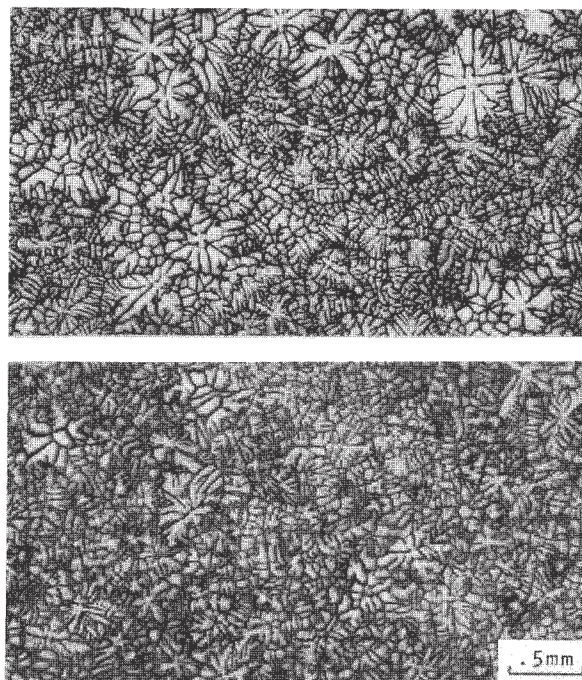


Figure 2. Effect of casting speed on dendrite structure at the center of 2024 billets cast with 660°C metal temperature and 550 l/min water flow. Upper: R = 6.35 cm/min; lower: R = 3.8 cm/min.

billets. The dendrite arm spacing at this location was about equal to that of the background structure in the center of the billets cast at the faster speed (the solidification rates were also about the same -- Table I).

Grain sizes at the D/4 position were somewhat finer than those at the center, and the billets cast with the lower superheat were a little coarser than those cast with 715°C metal (Fig. 4). Casting speed and water flow had no significant effect on grain size.

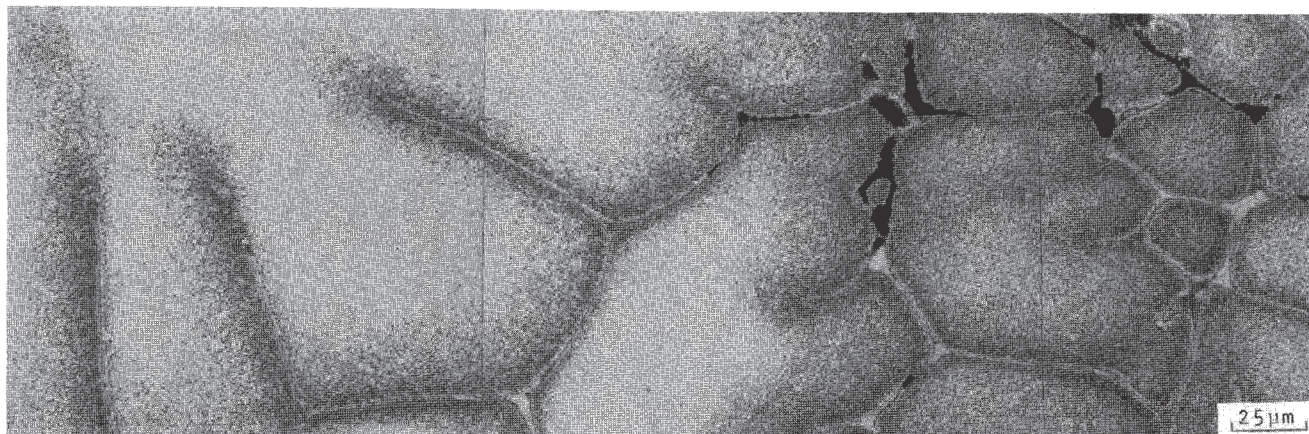


Figure 3. Microstructure variation across coarse dendrite structure in center of 2024 billet cast at 6.35 cm/min with 660°C metal temperature and 550 l/min water flow.

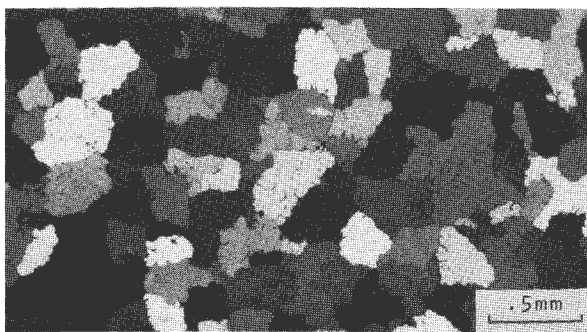
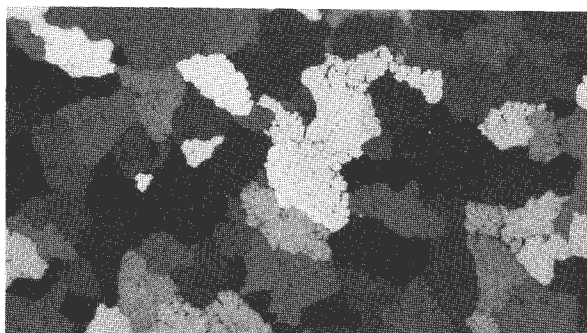


Figure 4. Grain structure at D/4 position in billets cast at 3.8 cm/min and 550 l/min water flow. Upper: 660°C metal temperature; lower: 715°C.

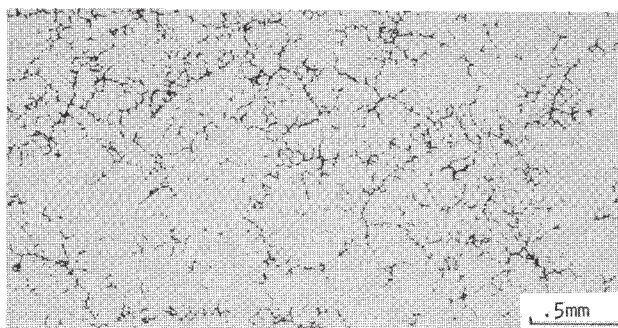
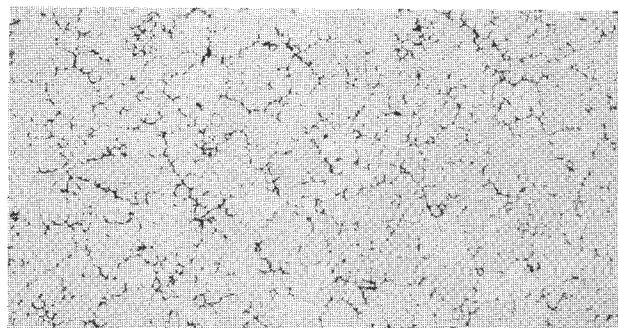


Figure 5. Constituent distribution at the center of homogenized 2024 billets (550 l/min water flow). Upper: R = 3.8 cm/min, 715°C metal temperature; lower: R = 6.35 cm/min, 660°C metal temperature.

After a 495°C homogenization treatment, a considerable amount of constituent remained (Fig. 5), and it was more heterogeneously distributed in billets cast at the faster drop rate, even at the D/4 position. Since the average compositions are about the same at the D/4 position, the constituent-enriched regions in the 6.35 cm/min billet are probably more concentrated than those in billet cast at the slower rate. The actual phases in the billets as identified by optical microscopy (Fig. 6), were $\alpha\text{Al}(\text{Fe},\text{Mn})\text{Si}$, $\text{Al}_7\text{Cu}_2\text{Fe}$, CuAl_2 and Al_2CuMg .

Differential Scanning Calorimetry (DSC)

The volume fraction of undissolved "soluble" phases Al_2CuMg and CuAl_2 can be estimated indirectly by differential scanning calorimetry. Prior work has shown that the total amount of constituent in 2024 alloy can be approximated by⁽²⁾

$$\text{Vol. \%} \approx 10(\% \text{Fe}) + 0.50E + 0.075E^2$$

where E is the melting energy (cal/g) of the "ternary" and "binary" eutectics comprised of Al matrix, Al_2CuMg and CuAl_2 . The %Fe term accounts

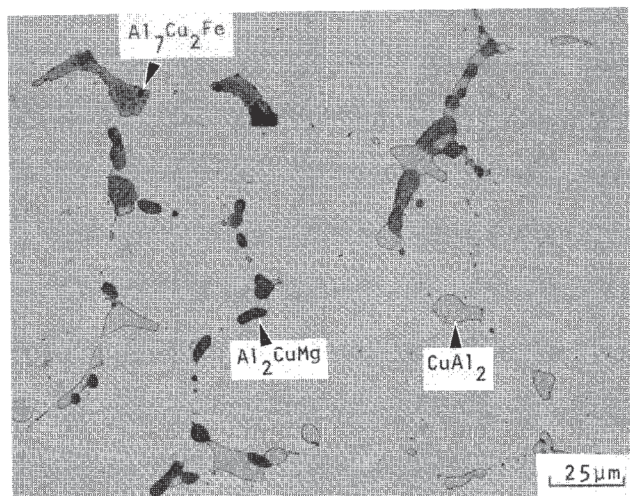


Figure 6. Microstructure of homogenized 2024 billet.

for the relatively insoluble phases α AlFeSi and Al_7Cu_2Fe .

The effect of the 16 h homogenization treatment at 495°C on the melting peak is shown in Figure 7. The observed reduction in melting energy (6.93 to 1.95 cal/g) suggests a 3-fold decrease in the total amount of second phase constituents. Higher definition examples of melting peaks in the homogenized material are shown in Figure 8. There were two distinct melting peaks, the first presumably due to the ternary $CuAl_2 + Al_2CuMg + Al$ eutectic, and the second the binary $CuAl_2 + Al$ eutectic.

Table IV gives a comparison of the melting energies and estimated constituent levels in two billets cast under different conditions (deep isothermal sump vs. shallow high-gradient sump). In the latter material the as-cast D/2 peak was greater than that at the D/4 position (matches chemistry), but the situation reversed after homogenization. This suggests that the slower casting speed produces a microstructure that is more "homogenizable". It is also apparent that the slower casting speed produced a more uniform constituent distribution across the billet diameter, as well as a more locally uniform microstructure (Fig. 5).

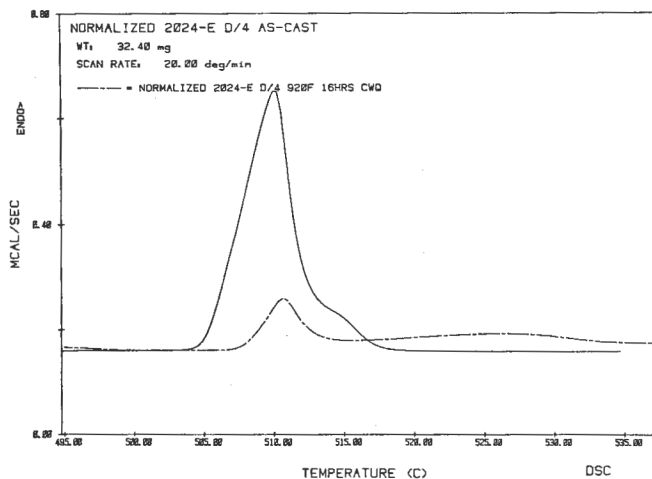


Figure 7. Normalized DSC thermograms from the D/4 position in stress relieved (solid) line and homogenized (dashed line) 2024 billet cast at 6.35 cm/min using 660°C metal temperature.

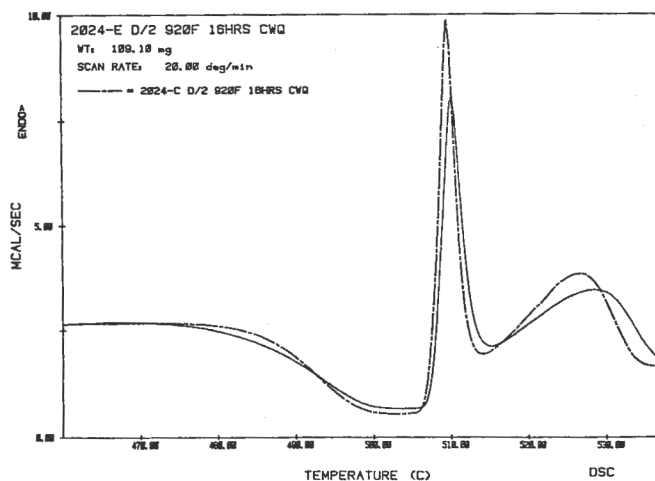


Figure 8. DSC thermograms from the D/2 position in homogenized 2024 billets. Solid line: $R = 6.35$ cm/min, 660°C metal temperature; dashed line: $R = 3.8$ cm/min, 715°C metal temperature.

Table IV. DSC Data for As-Cast and Homogenized 2024 Billets: 505-535F Melting Peaks

| Casting Speed (cm/min) | Metal Temp. (°C) | Condition | Energy (cal/g) | | Vol. % Total Constituent ^a | | |
|------------------------|------------------|-----------|----------------|------|---------------------------------------|------|----------|
| | | | D/4 | D/2 | D/4 | D/2 | Δ |
| 6.35 | 660 | As-Cast | 6.93 | 6.39 | 9.06 | 8.25 | 0.80 |
| | | Homog. | 1.95 | 1.56 | 3.26 | 2.96 | 0.30 |
| 3.8 | 715 | As-Cast | 6.91 | 7.30 | 9.04 | 9.65 | -0.61 |
| | | Homog. | 1.85 | 1.68 | 3.18 | 3.05 | 0.13 |

^a Estimated from DSC melting energy; 0.2% Fe contributes ~2.0% constituent as α AlFeSi and Al_7Cu_2Fe .

Discussion

This study has shown good qualitative agreement between casting practice, macrosegregation and microstructure of 2024 billet. Practices that promote a deep sump (fast casting speed) provide the conditions for collection of large solute-depleted "isothermal" dendrites, resulting in the typical macrosegregation profiles normally observed in DC cast ingots⁽⁴⁾, i.e., low concentrations of alloying elements at the ingot center. This situation appears to be accentuated by an isothermal sump (low metal superheat). The effects of mold water flow are secondary, but may be contributory under low superheat - fast drop rate conditions, i.e., low water flow relates to more macrosegregation.

Casting practices that give a shallow sump (slow drop rate) generate an unusual (but flatter) segregation profile, in which the concentration of alloying elements can be higher at the ingot center than at the quarter point. Although high metal superheat increases sump depth slightly, it appears beneficial from a macrosegregation viewpoint because it is less conducive to the formation of isothermal solute-depleted primaries.

Conditions that lead to macrosegregation result in a heterogeneous microstructure in the alloy-depleted regions. First, the dendrite arm spacing has a bimodal distribution because the isothermal primaries have a much coarser structure (slower solidification rate) than the metal that freezes "in situ". Second, the distribution of constituent is very non-uniform because the isothermal primaries are solute depleted. And, this localized heterogeneity persists after homogenization since a great deal of the constituent (Al_7Cu_2Fe and $\alpha AlFeSi$) is insoluble. The same conditions that lead to localized heterogeneities also promote non-uniform microstructures across the billet diameter. The total amount of constituent, as well as its distribution, is more uniform in billet cast under conditions that favor relatively shallow, high-gradient sumps.

Conclusions

Casting conditions that favor high solidification rates do not necessarily produce desirable microstructures. For example, high casting speeds, which promote deep liquid metal sumps, lead to the collection of coarse solute-depleted "isothermal" dendrites in the center of the ingot. This results in heterogeneous duplex microstructures, which persist even after homogenization.

References

1. E. D. Tarapore, "Thermal Modeling of DC Continuous Billet Casting," *Light Metals 1989*, ed. P. G. Campbell (Warrendale, PA: TMS-AIME), 875-880.
2. D. J. Beerntsen and K. R. Brown, "Determination of Volume of Excess Soluble Phases and Solution Treatment Temperature of 2X24 Type Aluminum Alloys by DSC," (Paper presented at the 3rd Int. Conf. on Progress in Microstructure, Aachen, W. Germany, May, 1987).
3. R. E. Spear and G. R. Gardner, "Dendrite Cell Size," *A.F.S. Trans.*, 71 (1963), 209-215.
4. H. Yu and D. A. Granger, "Macrosegregation in Aluminum Alloy Ingot Cast by the Semicontinuous Direct Chill Method," *Fundamentals of Alloy Solidification Applied to Industrial Processes*, NASA Symposium, 1984, 157-168.